




Numerical Analysis of Two-Phase Flow in Serrated Minichannels Using COMSOL Multiphysics

Razieh Abbasgholi Rezaei^{1*} 

Department of Mechanical Engineering, Urmia University, 5756151818 Urmia, Iran

* Correspondence: Razieh Abbasgholi Rezaei (r_rezaei_mec@yahoo.com)

Received: 10-14-2023

Revised: 11-21-2023

Accepted: 11-29-2023

Citation: R. A. Rezaei, "Numerical analysis of two-phase flow in serrated minichannels using COMSOL multiphysics," *J. Ind Intell.*, vol. 1, no. 4, pp. 194–202, 2023. <https://doi.org/10.56578/jii010401>.



© 2023 by the authors. Licensee Acadlore Publishing Services Limited, Hong Kong. This article can be downloaded for free, and reused and quoted with a citation of the original published version, under the CC BY 4.0 license.

Abstract: In the realm of engineering, the significance of minichannels has escalated, especially in micro-scale multiphase fluid dynamics. This study conducts an extensive numerical analysis of two-phase flow in minichannels, utilizing the level-set method coupled with COMSOL Multiphysics®. Focusing on the minutiae of the liquid-gas interface, the research employs a two-dimensional grid to solve the incompressible Navier-Stokes equations, thereby illuminating the complex formation of diverse flow patterns in minichannels. A critical aspect of this investigation is the exploration of various geometric configurations at the inlet, particularly the examination of serrated air and water inlet channels. The findings reveal that serrated air inlets, when designed internally, effectively mitigate the buoyancy force across diverse channel configurations, ensuring stable and predictable flow patterns. Conversely, the configuration of water inlets plays a less significant role in controlling this force, underscoring the paramount importance of air inlet design in achieving optimal flow regulation. These insights not only deepen the understanding of minichannel flow dynamics but also provide practical knowledge for enhancing the efficiency of micro-scale systems. The implications of this study extend to the design of more effective minichannel applications, such as cooling systems, heat sinks, and heat exchangers used as evaporators. Moreover, the research highlights the necessity of considering geometric factors in minichannel flow analyses and sets the stage for future advancements in this evolving domain of engineering.

Keywords: Two-phase flow; Minichannel; Liquid-gas interface; COMSOL multiphysics; Level-set function; Serrated inlet

1 Introduction

In the contemporary landscape of microscale fluid dynamics, the exploration of two-phase flow in miniaturized channels has garnered significant attention. The proliferation of minichannels in applications such as heat exchangers and chemical reactors has catalyzed a surge in both experimental and numerical studies aimed at elucidating the complexities of two-phase flow phenomena. It has been recognized that Computational Fluid Dynamics (CFD) offers a robust framework for simulating these intricate multiphase flows. However, the accurate representation of fluid interface behavior remains a pivotal challenge in this domain.

The dynamic motion of fluid interfaces has been the subject of extensive research, with numerous numerical techniques proposed, spanning both Lagrangian and Eulerian approaches. Lagrangian methods, which track interface movement via markers, contrast sharply with Eulerian techniques that define the interface as a specific isocontour of a globally defined function. Notably, Eulerian approaches have been favored due to inherent advantages in managing complex interface dynamics [1–3]. Among Eulerian techniques, the level-set method stands out for its versatility and efficacy [4–6]. This method, employed in a wide array of fields including computational fluid dynamics, computer graphics, and shape optimization, relies on a mathematical function that captures the geometric properties of evolving interfaces as an implicit surface [7–10]. Its proficiency in tracking and rendering the motion of intricate shapes and handling topological transformations, like interface merging and splitting, is unparalleled [11–15]. Furthermore, the level-set method is adept at managing evolving geometries with high accuracy and computational efficiency, making it a preferred choice in diverse scientific applications [16–19].

This study delves into the influence of various geometric factors in the inlet section of a minichannel on two-phase flow patterns. Employing the level-set method within COMSOL Multiphysics, the investigation seeks to unveil how

different geometric configurations impact the dynamics and characteristics of two-phase flow. The insights gleaned from this analysis are anticipated to significantly enhance our understanding of minichannel flows and contribute to the advancement of miniaturized device design, promising improved efficiency and performance.

2 Numerical Implementation

The COMSOL Multiphysics software was employed for the numerical implementation, involving the solution of the Navier-Stokes equations in conjunction with a level-set function. The level-set function, represented as follows:

$$\rho(u \cdot \nabla)u = \nabla \cdot [-pI + \mu(\nabla u + (\nabla u)^T)] + F, \rho \nabla \cdot u = 0$$

where, ρ , u , p , and I denote density, velocity, pressure, and matrix, respectively.

The minichannel under study, with dimensions of 200mm in length and 3mm in height, was modeled to include two water inlets and a singular air inlet. The air inlet was positioned strategically between the two water inlets, as depicted in Figure 1. Figure 1 illustrates the inlet boundaries for water and air in blue lines. This study's focal point includes the analysis of various configurations of serrated minichannels at the inlets, as demonstrated in Figure 2.

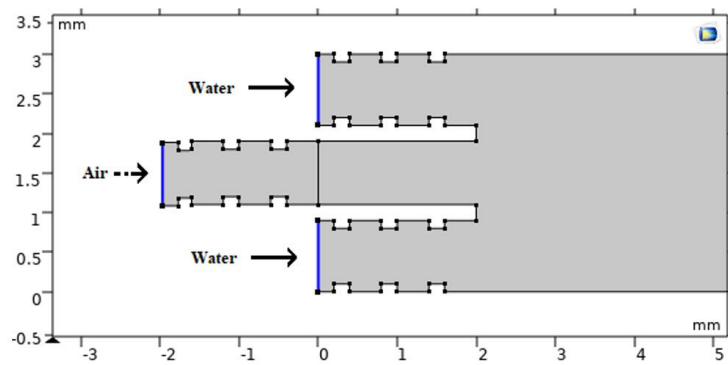


Figure 1. Inlet fluides of the minichannel

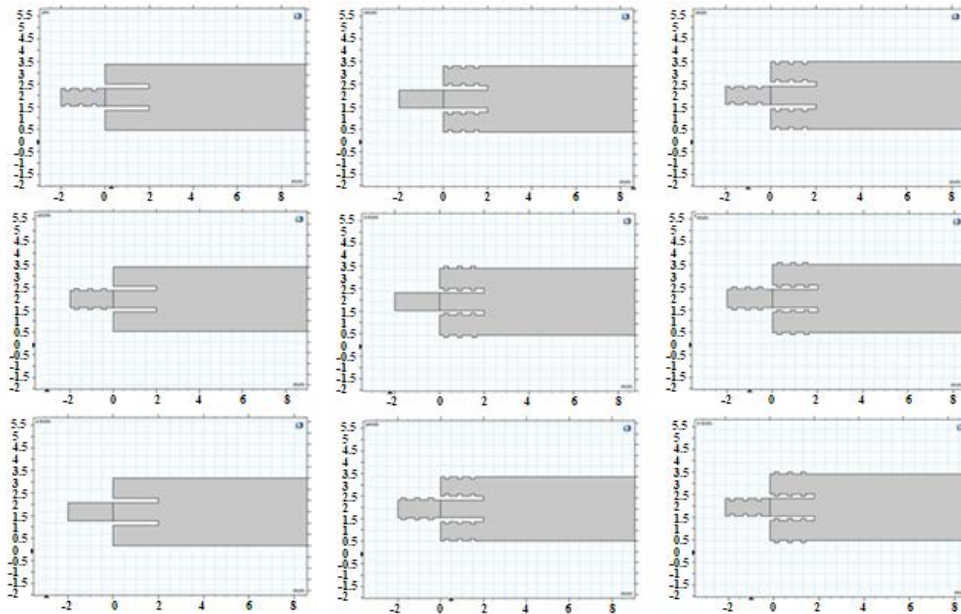


Figure 2. Various arrangements of the studied inlet serrated minichannel

Velocity profiles of the inlet air and water flows are presented in Figure 3. Here, the inlet fluid velocities are normalized per length of the boundary, converting them into a dimensionless form for ease of comparison across different boundary points. The boundary conditions for the inlets were established as ‘velocity’, signifying pre-defined velocities for the fluids at these points. These velocities, set as initial conditions, are independent of the fluid flow dynamics within the system. Table 1 details the specific velocity values assigned to the inlets. Conversely, the boundary condition at the outlet was designated as ‘pressure’, with a prescribed pressure set to 0Pa.

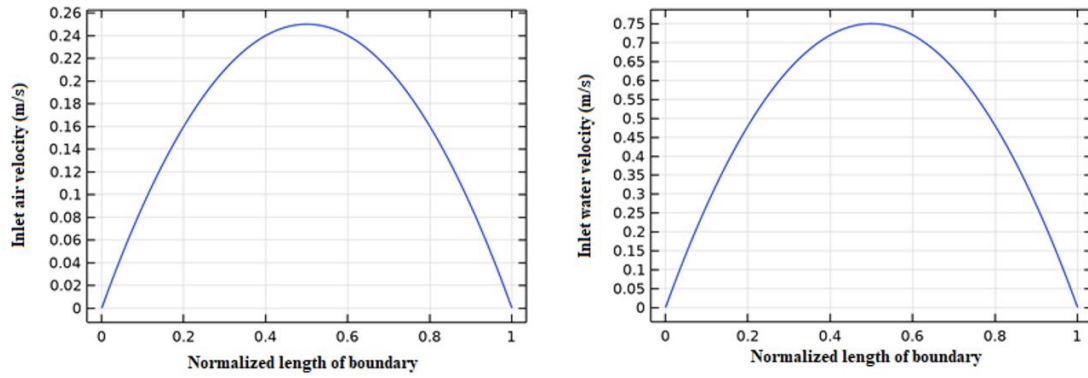


Figure 3. Velocity profiles of the inlet air and waters flows

Table 1. Inlet velocities

Description	Value	Unit
Normal water inflow velocity	0.2	m/s
Normal air inflow velocity	0.5	m/s

In establishing the boundary conditions for the walls within the simulation, different types were considered. The walls depicted in Figure 4A were designated as ‘no-slip’ boundaries. This classification implies that the fluid in direct contact with these walls adheres strictly to them, resulting in a zero velocity at the wall surface. Essentially, the fluid adjacent to these walls remains stationary, not exhibiting any movement along the wall’s surface. On the other hand, the walls shown in Figure 4B were classified as ‘no-flow’ boundaries, indicating the absence of fluid flow across these walls. Additionally, the contact angle between the fluid and the wall surface was set at 20 radians. This angle, defined as the angle between the fluid surface and the tangent to the wall surface at the point of contact, was consistently maintained at 20 radians.

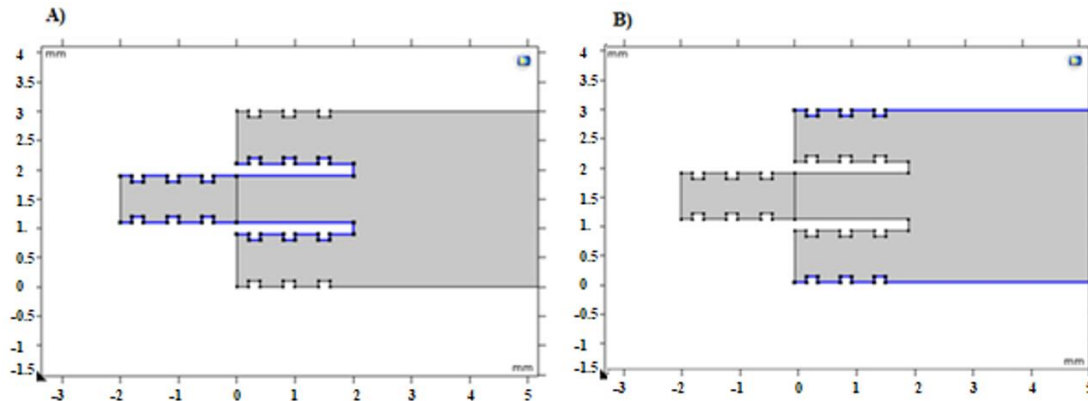


Figure 4. Boundary conditions for walls; A) No-slip boundary, B) No-flow boundary

Figure 5 delineates the respective domains of air and water within the computational model. It also highlights the initial interface boundary, marked in red, representing the initial demarcation between the air and water phases at the commencement of the simulation.

The study employed a physics-controlled mesh, where the mesh resolution was specifically tailored to the underlying physical phenomena of the problem. This approach entailed utilizing a finer mesh in areas of significant physical property variations or gradients, thereby enhancing precision in regions of interest. Conversely, in zones where these variations were minimal or less critical for the analysis, a coarser mesh was utilized. This strategy effectively balanced computational efficiency with accuracy. Figure 6 showcases the physics-controlled mesh near the minichannel inlets, which was integral to the study. The total number of mesh elements utilized amounted to 15,521. Table 2 presents the mesh statistics related to the physics-controlled mesh used in this study. Figure 6 illustrates the structured grid elements in specific regions, dictated by the physics-based criteria.

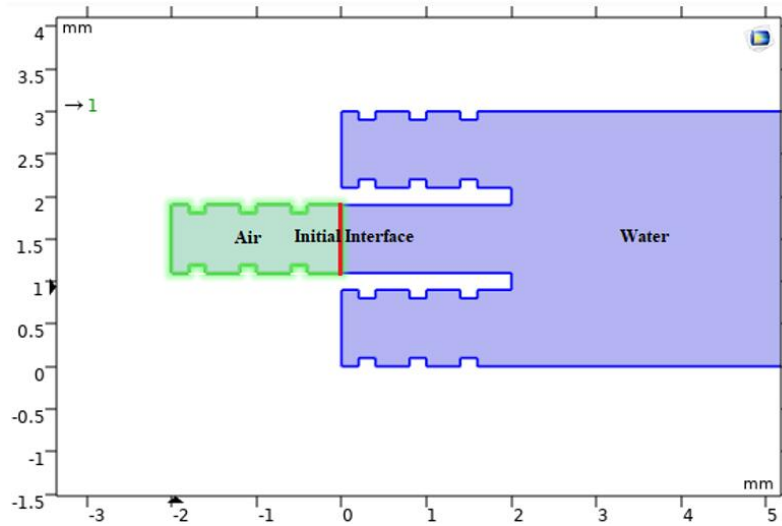


Figure 5. Domains and initial interface

Table 2. Mesh statistics

Description	Value
Mesh vertices	8475
Triangles	15425
Quads	96
Edge elements	1338
Vertex elements	14
Number of elements	15521
Minimum element quality	0.2012
Average element quality	0.9452
Element area ratio	0.0080062
Mesh area	600.8 mm ²

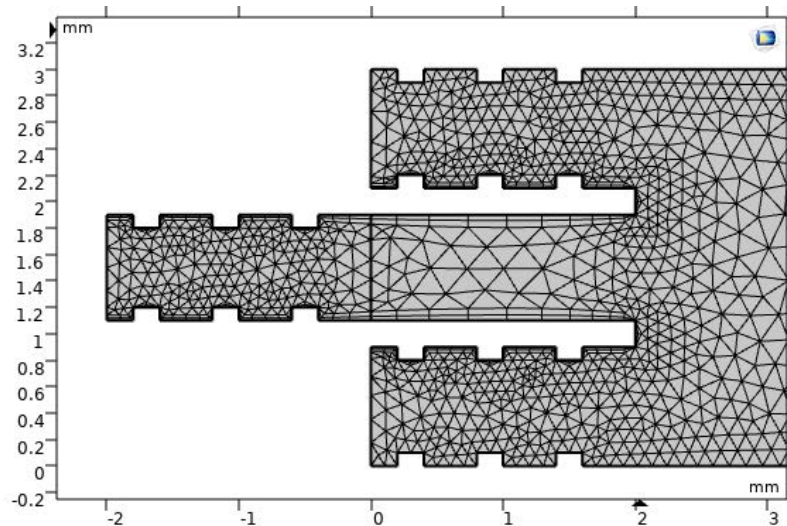


Figure 6. Grid elements structured in certain regions as dictated by the physics-based criteria

Validation and Verification

The validation and verification of the numerical solutions obtained using COMSOL Multiphysics are pivotal to ensure their accuracy and reliability. Validation entails the comparison of numerical results with experimental data or analytical solutions from benchmark studies. It is instrumental in confirming the fidelity of the simulation outcomes. Verification, conversely, is centered on evaluating the convergence and consistency of the numerical

methods implemented. These procedures are crucial for establishing confidence in the simulation results and affirming the capability of the software to address complex fluid flow challenges.

In the context of this study, the results pertaining to bubble formation within a minichannel with a straight inlet ($U_{\max, \text{water}} = 0.2 \text{ [m.s}^{-1}\text{]}$, $U_{\max, \text{air}} = 0.5 \text{ [m.s}^{-1}\text{]}$) were compared against the findings of Grzybowski and Mosdorf [20]. This comparison, as illustrated in Figure 7, demonstrates a high degree of concordance. Figure 7A showcases the bubble formation inside the straight minichannel at different time frames (0.04, 0.32, 0.76, and 1.2 seconds) as simulated in this study. Correspondingly, Figure 7B displays the bubble formation under similar conditions as simulated by Grzybowski and Mosdorf [20].

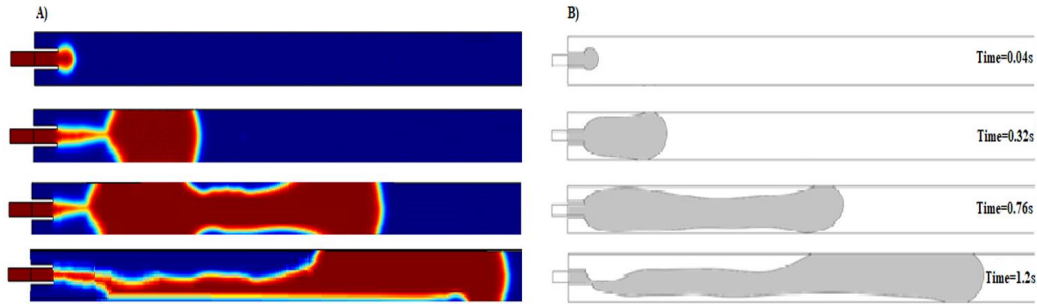


Figure 7. Bubble formation inside the straight minichannel at various time frames: A) Analyzed in the present study, B) Analyzed by Grzybowski and Mosdorf [20]

In the results section, the magnitudes of velocities and the volume fractions of water and air fluids at specific time intervals (0.1, 0.2, 0.3, and 0.5 seconds) in assumed channel configurations with varying inlet designs will be examined.

3 Results

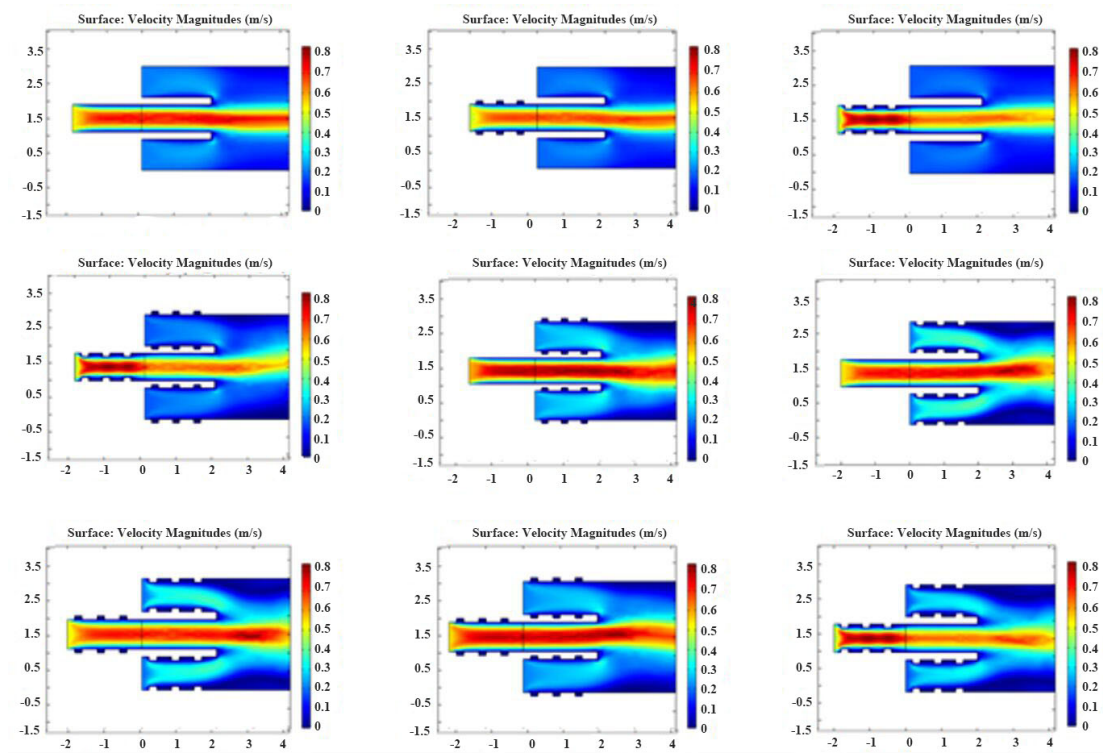


Figure 8. Velocity magnitudes in assumed channel configurations

Figure 8 delineates the velocity comparisons across various channel configurations. It was observed that the outside staggered channels exhibited higher velocities relative to the straight channels, a phenomenon attributable to vortex formation caused by abrupt changes in surface area through which the fluid travels. These vortices

significantly contribute to increased velocities in the outside staggered channels, with a recorded increment of 65.2% and 32.72% for water and air inlets, respectively, when compared to the velocities in straight channels. Notably, the highest velocity was recorded in the inside staggered channels, which surpassed both straight and outside staggered configurations in terms of flow velocity.

Figure 9 presents the volume fractions of fluids at specified time intervals (0.1s, 0.2s, 0.3s, and 0.5s) for three distinct inlet channel configurations: totally inside serrated, totally outside serrated, and straight channels. In the scenarios involving totally outside serrated and straight inlet channels, it was observed that the slugs formed were influenced by buoyancy forces, leading to their upward movement within the channel. This ascent is primarily due to density differentials between the fluids, engendering buoyancy effects. However, in the case of totally inside serrated inlet channels, the elevated fluid velocities were found to counteract the buoyancy forces. Consequently, the higher flow velocity within the totally inside serrated channels effectively mitigated the upward movement of slugs induced by buoyancy.

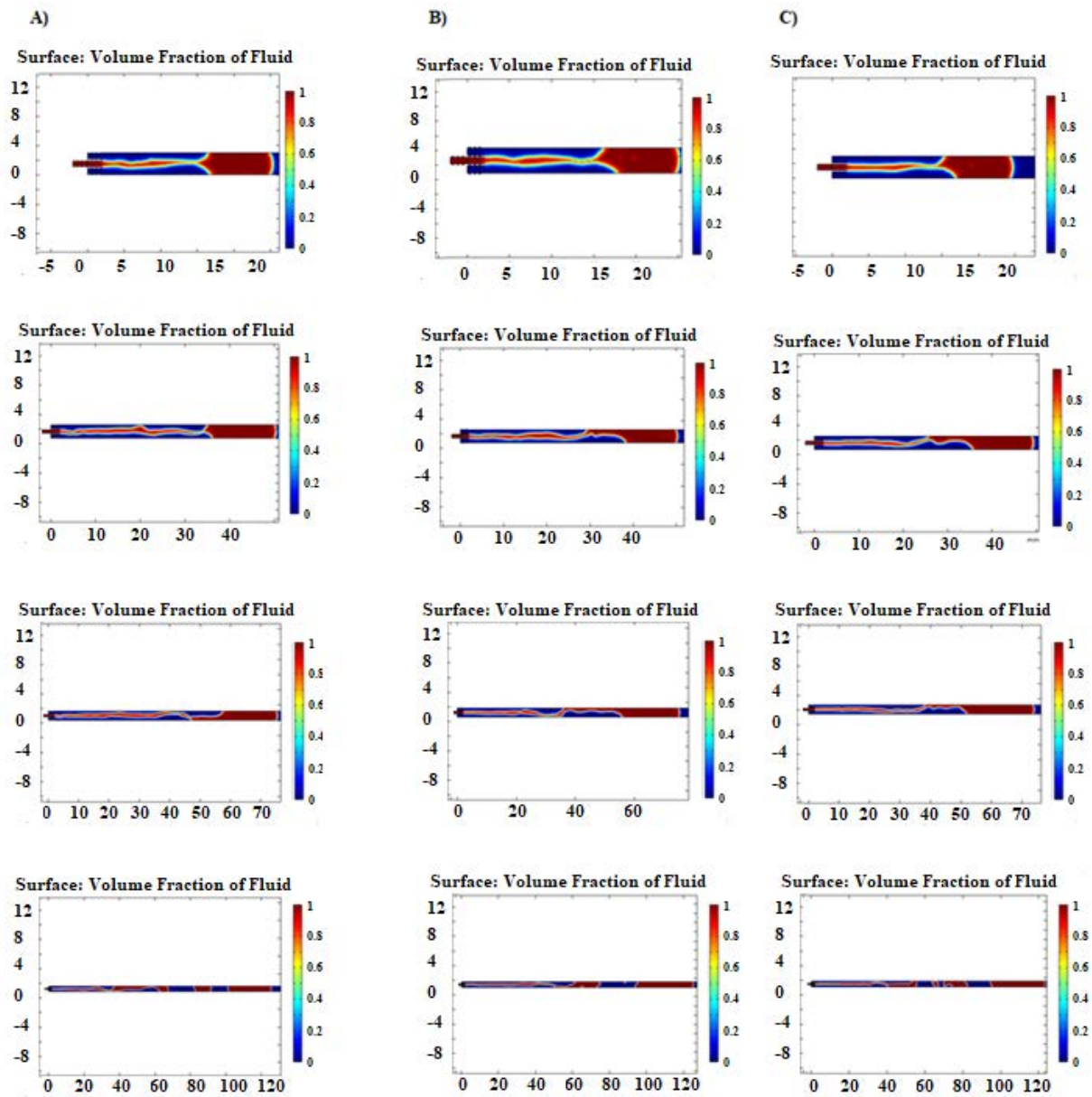


Figure 9. Volume fractions of fluids at specific time intervals (0.1s, 0.2s, 0.3s, and 0.5s) for three different inlet channel configurations: A) totally inside serrated, B) totally outside serrated, and C) totally straight channels

The efficacy of the air inlet with an inside serrated design was meticulously analyzed across all geometries incorporating this specific inlet shape, as depicted in Figure 10. Figure 10 exhibits scenarios where the air inlet is inside serrated, and the water inlets are, respectively, straight, outside serrated, and inside serrated. A noteworthy

finding from these illustrations is the consistent mitigation of buoyancy force by the inside serrated air inlet across all geometries. This observation underscores the predominant role of the inside serrated air inlet design in counteracting buoyancy effects, irrespective of the water inlet shape. Figure 10 showcases the channels with an inside serrated air inlet and various water inlet designs at a time interval of 0.3 seconds. A critical insight gained is the longer duration of slug formation in the totally inside serrated channel prior to the onset of separation, in contrast to the shorter slug durations observed in other configurations. Specifically, the slug in the totally inside serrated channel persisted for 78mm, approximately 28mm longer than that in other channel designs.

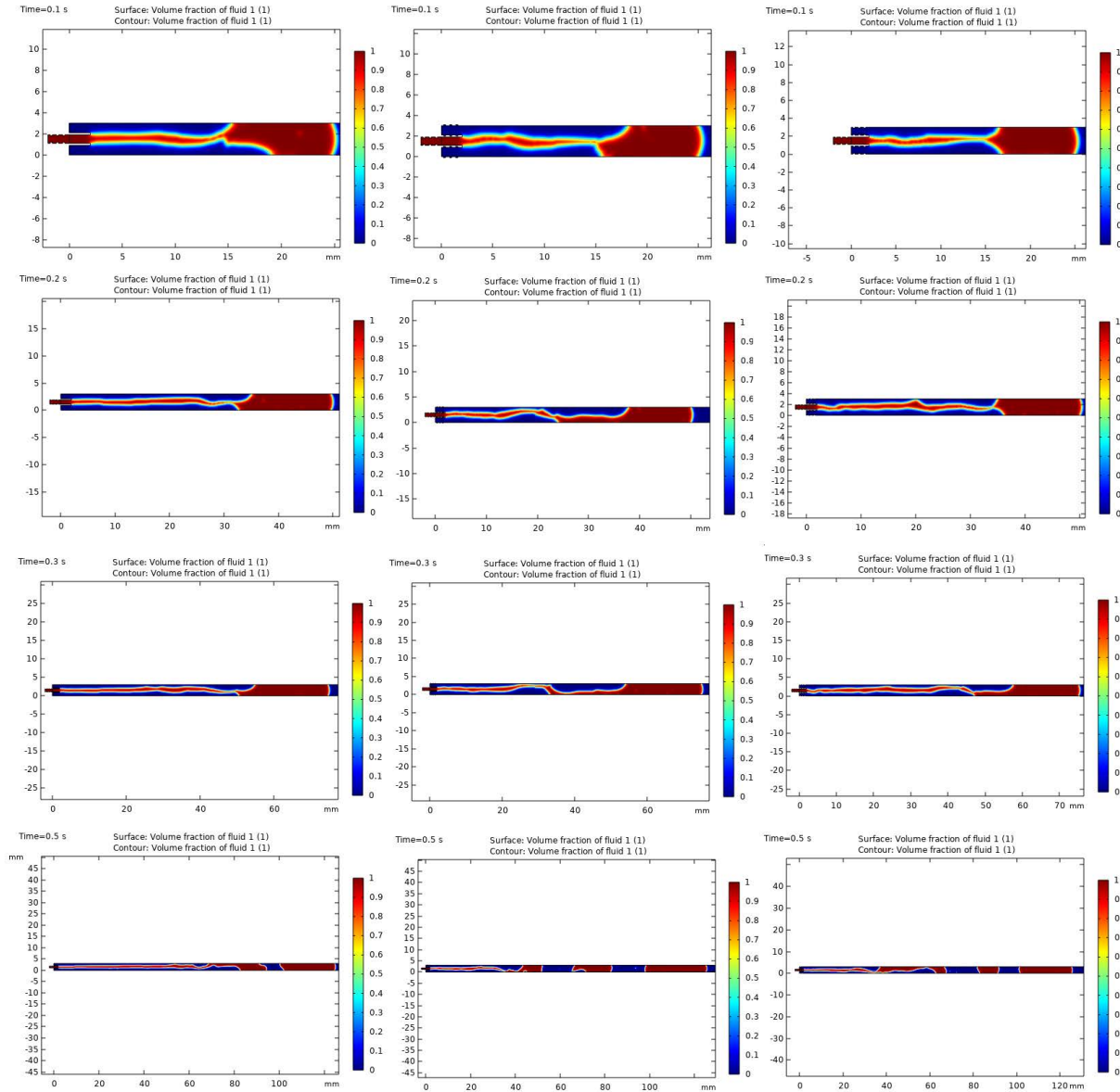


Figure 10. Channels with inside serrated air inlet and various water inlet shapes at 0.3s time interval

4 Conclusions

The investigation conducted in this study meticulously explored the influence of various geometric factors in the inlet sections of minichannels on the complex dynamics of two-phase flow. Utilizing the level-set method within COMSOL Multiphysics, an extensive analysis was performed, focusing on velocity profiles and fluid volume fractions across different time intervals in three distinct inlet channel configurations. The results yielded significant insights:

- Inside staggered channels were observed to exhibit the highest flow velocities among the tested configurations, surpassing both straight and outside staggered channels.
- A pronounced increase in velocities was recorded in outside staggered channels, showing an enhancement of

65.2% and 32.72% for water and air sections, respectively, compared to straight channels.

- The application of an inside serrated air inlet design was found to effectively suppress buoyancy forces across all channel configurations.

- Contrary to initial expectations, the shape of the water inlet appeared to play a minimal role in mitigating the buoyancy force.

- The most extended slug duration prior to separation was noted in the totally inside serrated channel configuration, particularly evident at the 0.3s time interval.

These findings contribute to a more profound understanding of minichannel flow dynamics, offering valuable insights into two-phase flow behaviors under various geometric conditions. Such knowledge is particularly beneficial for industrial applications in liquid cooling systems, heat sinks, and minichannel heat exchangers used as evaporators. The negligible impact of water inlet shape on buoyancy force mitigation emerged as a surprising result, warranting further investigation to corroborate this observation.

Data Availability

The data used to support the findings of this study are available from the corresponding author upon request.

Conflicts of Interest

The author declares no conflict of interest.

References

- [1] K. Museth, D. E. Breen, R. Whitaker, and A. H. Barr, “Level set surface editing operators,” *ACM Trans. Graph.*, vol. 21, no. 3, pp. 330–338, 2002. <https://doi.org/10.1145/566654.566585>
- [2] A. Soulaïmani and Y. Saad, “An arbitrary Lagrangian-Eulerian finite element method for solving three-dimensional free surface flows,” *Comput. Meth. Appl. Mech. Eng.*, vol. 162, no. 1-4, pp. 79–106, 1998. [https://doi.org/10.1016/s0045-7825\(97\)00330-7](https://doi.org/10.1016/s0045-7825(97)00330-7)
- [3] M. Droske and M. Rumpf, “A level set formulation for Willmore flow,” *Interfaces Free Bound.*, vol. 6, pp. 361–378, 2004. <https://doi.org/10.4171/ifb/105>
- [4] S. Alizadeh and R. A. Rezaei, “Numerical analysis of viscosity and surface tension on microdroplet dynamics in microelectromechanical systems applications,” *J. Ind. Intell.*, vol. 1, no. 3, pp. 158–164, 2023. <https://doi.org/10.56578/jii010303>
- [5] P. Frolkovic and K. Mikula, “High-resolution fluxbased level set method,” *SIAM J. Sci. Comput.*, vol. 2005, no. 29, p. 2, 2005. <https://doi.org/10.1137/05064656>
- [6] S. Osher and J. A. Sethian, “Fronts propagating with curvature-dependent speed: Algorithms based on Hamilton-Jacobi formulations,” *J. Comput. Phys.*, vol. 79, no. 1, pp. 12–49, 1988. [https://doi.org/10.1016/0021-9991\(88\)90002-2](https://doi.org/10.1016/0021-9991(88)90002-2)
- [7] S. E. Hieber and P. Koumoutsakos, “A Lagrangian particle level set method,” *J. Comput. Phys.*, vol. 210, no. 1, pp. 342–367, 2005. <https://doi.org/10.1016/j.jcp.2005.04.013>
- [8] S. Osher and R. Fedkiw, *Level Set Methods and Dynamic Implicit Surfaces*. Springer, New York, USA, 2003.
- [9] R. A. Rezaei, “Experimental investigation on the performance of circumferential corrugations helical tubes based on thermodynamic and economic analyses,” *Proceedings of the Institution of Mechanical Engineers, Part C: Journal of Mechanical Engineering Science*, vol. 237, no. 6, pp. 1499–1509, 2023. <https://doi.org/10.1177/09544062221130210>
- [10] W. J. Rider and D. B. Kothe, “Reconstructing volume tracking,” *J. Comput. Phys.*, vol. 141, no. 2, pp. 112–152, 1998. <https://doi.org/10.1006/jcph.1998.5906>
- [11] B. Houston, M. B. Nielsen, C. Batty, O. Nilsson, and K. Museth, “Hierarchical RLE level set,” *ACM Trans. Graph.*, vol. 25, no. 1, pp. 151–175, 2006. <https://doi.org/10.1145/1122501.1122508>
- [12] P. Chiu and Y. Lin, “A conservative phase field method for solving incompressible two-phase flows,” *J. Comput. Phys.*, vol. 230, no. 1, pp. 185–204, 2011. <https://doi.org/10.1016/j.jcp.2010.09.021>
- [13] Y. Sun and C. Beckermann, “Sharp interface tracking using the phase-field equation,” *J. Comput. Phys.*, vol. 220, no. 2, pp. 626–653, 2007. <https://doi.org/10.1016/j.jcp.2006.05.025>
- [14] A. Mukherjee, S. G. Kandlikar, and Z. J. Edel, “Numerical study of bubble growth and wall heat transfer during flow boiling in a microchannel,” *Int. J. Heat Mass Trans.*, vol. 54, no. 15-16, pp. 3702–3718, 2011. <https://doi.org/10.1016/j.ijheatmasstransfer.2011.01.030>
- [15] J. H. Ferziger, “Interfacial transfer in Tryggvason’s method,” *Int. J. Numer. Meth. Fluids*, vol. 41, no. 5, pp. 551–560, 2003. <https://doi.org/10.1002/flid.455>
- [16] COMSOL, “Comsol Multiphysics Reference Manual.” https://doc.comsol.com/5.5/doc/com.comsol.help.comsol/COMSOL_ReferenceManual.pdf

- [17] H. Sheykhlou, S. Jafarmadar, and R. A. Rezaei, "Exergy analysis of novel integrated systems based on MHD generators," *Int. J. Exergy*, vol. 35, no. 1, p. 3, 2021. <https://doi.org/10.1504/ijex.2021.115081>
- [18] O. A. Odumosu, H. Xu, T. Wang, and Z. Che, "Growth of elongated vapor bubbles during flow boiling heat transfer in wavy microchannels," *Appl. Therm. Eng.*, vol. 223, p. 119987, 2023. <https://doi.org/10.1016/j.applthermaleng.2023.119987>
- [19] G. Yang, W. Zhang, M. Binama, J. Sun, and W. Cai, "Review on bubble dynamic of subcooled flow boiling-Part A: Research methodologies," *Int. J. Therm. Sci.*, vol. 184, p. 108019, 2023. <https://doi.org/10.1016/j.ijthermalsci.2022.108019>
- [20] H. Grzybowski and R. Mosdorf, "Modelling of two-phase flow in a minichannel using level-set method," *J. Phys. Conf. Ser.*, vol. 530, p. 012049, 2014. <https://doi.org/10.1088/1742-6596/530/1/012049>